RESEARCH ARTICLE

Macromolecular Rapid Communications
www.mrc-journal.de

Heating Rate Sensitive Polyethylene Terephthalate

*Robert David Ludwig Jerusalem, Michail Maricanov, Thomas Raidt, Frank Katzenberg, and Joerg Christian Tiller**

Smart materials react to external triggers by changing size, color, mechanical properties, or permeability. The next generation of smart materials will be able to not only recognize and react to external triggers but also to their dynamics. The only existing example of such a material is heating rate-sensitive polymorphous cross-linked syndiotactic polypropylene. This study presents a new principle of a heating rate-sensitive material on the example of cross-linked and fully amorphous quenchable semi-crystalline polyethylene terephthalate (x-PET). The x-PET is stretched to high elongation above its melting temperature and constrained quenched to a fully amorphous state. Then the polymer is heated to 120–170 °C with different heating rates. Due to its heating-rate sensitivity, x-PET shrinks to different stabilized lengths dependent on the heating rate. The new length can be used to read out the heating rate and to specifically answer to this by mechanically switching a process. Detailed analytics of this process reveal that amorphous stretched x-PET is starting the retraction above T_g and simultaneously stopping it by crystallization. The different rates of these processes result in the heating rate sensitivity of x-PET.

1. Introduction

Polymeric smart materials can recognize a change in their environment and react to this by changing their properties. This makes them valuable in many applications such as diagnostics, tissue engineering, drug delivery, coatings, textiles, and microelectromechanical systems.[1] In the case of polymeric materials, this is typically achieved by a change in structure, induced by phase transitions like melting,[2] glass transition,[3,4] liquid crystal phase changes[5] or changes in basic chemical structures,[6] such as cis/trans isomerizations,[7,8] or reversible ring-opening.[9,10] These processes are triggered by changed external conditions, such as temperature,[11,12] moisture[3] or other solvent vapors,[13] or light.[14,15] These established systems can usually simply react to on- or off-switching of the external trigger. The next generation of smart materials will not only react to such states but will specifically react to dynamic changes of the external trigger. One example of the value of such materials is the reaction to heating rates, which is important whenever heating thermally unstable products. Here, precautions must be taken to avoid excessive heating rates and accidental overheating. The necessary monitoring and regulating of relevant process parameters usually requires complex systems comprising sensors and actuators with an electrical power supply. Principally, responsive materials such as shape memory polymers (SMPs) are an interesting option to autonomously solve this task, since they are capable of detecting and responding to many environmental changes without the need for any mechatronic or power supply.[16] The only example of such a material is x-sPP that realizes this through a change in crystal structure, which is rarely found in polymer systems.[17] Another conceivable more general approach to imprint the desired heating rate-sensitivity to an SMP could be based on semi-crystalline polymers that can be cross-linked and quenched to a fully amorphous state. Stretching such polymers to high elongation above their melting temperature and subsequent quenching below T_g under constrained conditions should stabilize them in a highly elongated state. The opposing interplay of relaxation and cold-crystallization processes, which sets in when the sample is reheated above T_g, could lead to the stabilization of the sample in an intermediate shape that desirably allows conclusions to be drawn about the previously applied heating rate. This novel concept can in principle be applied to many different polymers and thus addresses different and possibly even tunable temperature regions.

One prerequisite of achieving an efficient heating-rate sensitive actor is to use an SMP with high and recoverable stretchability. This can be best achieved by cross-linking high polymers near the gel point either covalently[18] or ionically[19] as previously shown in the example of polypropylene. Another requirement is that the retraction takes place in a broad temperature range, which is quite common for SMPs with the exception of shape memory natural rubber (SMNR).[20] The third aspect is that the polymer is crystallizing and has a glass transition above ambi-

R. D. L. Jerusalem, M. Maricanov, T. Raidt, F. Katzenberg, J. C. Tiller
Department of Biochemical and Chemical Engineering
Biomaterials & Polymer Science
TU Dortmund University
44221 Dortmund, Germany
E-mail: joerg.tiller@tu-dortmund.de

The ORCID identification number(s) for the author(s) of this article can be found under https://doi.org/10.1002/marc.202400346

DOI: 10.1002/marc.202400346

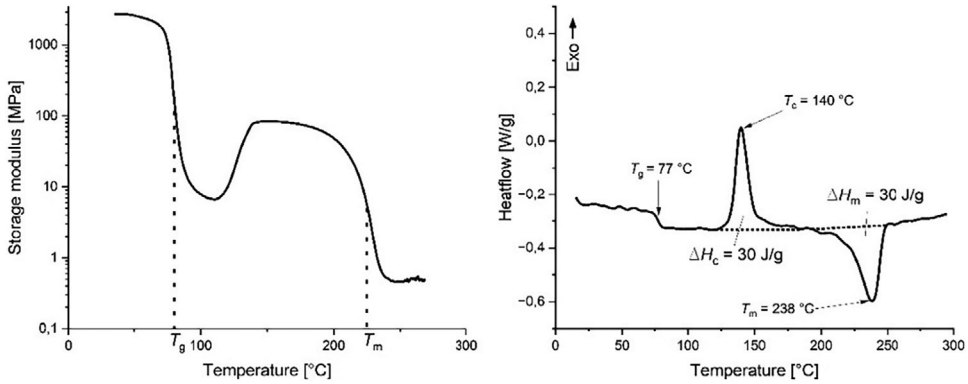

Figure 1. Storage modulus *E'* versus temperature *T* plot **(left)** and DSC plot **(right)** of an x-PET sample quenched from melt in ice water.

ent temperature, which is not influenced by cross-linking. Given these requirements, polyethylene terephthalate (PET), which can be critically crosslinked toward a high-temperature SMP,[21] was chosen as a promising system for this study.

2. Result

Polyethylene terephthalate (PET) was crosslinked following a recently published strategy by end group modification with phthalic anhydride (PA) followed by crosslinking with a tetra-arm epoxide (TGDDM). A Dynamic Mechanical Analyzer (DMA) was used to confirm the successful crosslinking of PET (x-PET). **Figure 1** (left) shows the storage modulus *E'* versus the temperature plot of an x-PET after being quenched from 290 °C in ice water.

As seen, the storage modulus *E'* drops significantly at the glass transition temperature (T_g), increases with the onset of cold crystallization, and drops down again after exceeding the melting temperature (T_m). The development of a stable plateau modulus above T_m confirms successful crosslinking of the prepared sample. The netchain molecular weight (M_c) was calculated to be 30.6 kg mol^{-1} according to Flory's theory of viscoelasticity (Equation 1), using the plateau modulus at 260 °C and a density of 1.18 g cm^{-3}.

Differential Scanning Calorimetry (DSC) was used to gain information about the remnant crystallinity of x-PET samples after being quenched from the melt. Figure 1 (right) reveals both a crystallization enthalpy ΔH_c of 30 J g^{-1} and a melting enthalpy ΔH_m of 30 J g^{-1} respectively, indicating that quenching of x-PET from 290 °C in ice water results in fully amorphous samples.

Next, it was investigated, if the crystallization of a highly elongated x-PET sample at 290 °C can be completely inhibited upon constrained quenching in ice water. Since the superposition of relaxation enthalpy with the melting enthalpy causes defective heat flows and prevents from any reliable evaluation, DCS could not be used for this. Therefore, wide-angle X-ray scattering (WAXS) was carried out with an x-PET sample heated to 290 °C at a hotplate, stretched to ϵ_{prog} = 200%, and immediately quenched in ice water, while keeping the stretching force constant. The recorded WAXS pattern (**Figure 3**, top left) shows an amorphous halo without any crystal reflections. Although small crystals may still be present, as WAXS is unable to detect crystals smaller than 5 nm,[22] constrained quenched x-PET samples were investigated regarding their heating rate sensitivity.

To this end, hot-stretched and constrained quenched x-PET samples were mounted to a film tension clamp of the DMA, and the length change was monitored against temperature for heating rates of 5, 10, and 20 K min^{-1}, respectively. **Figure 2** (left) shows the measured degree of recovery of x-PET samples constrained quenched from melt as a function of temperature and heating rate.

All samples show the typical triple-shape memory behavior with intermediate shapes strongly dependent on the applied heating rate. Thereby, the intermediate state is very stable and extends over a range of 100 K, which is superior to other literature-known multi-shape memory polymers, such as polyethylene,[23] PFSA,[24] or segmented PCL/PCHMA networks.[25] Expectedly, the recovery of the sample sets in when the glass transition temperature of ≈77 °C is exceeded. Cold crystallization starts delaying the recovery process from a temperature of ≈90 °C and ultimately stabilizes all x-PET samples in a heating-rate dependent intermediate shape until the melting temperature of the newly formed crystals of ≈200 °C is reached and the sample fully recovers its original dimensions. The investigated heating rates of 5, 10, and 20 K lead to intermediate forms at ≈20, 40, and 70% of the total recovery, whereby the temperature range in which the intermediate form is stable becomes somewhat smaller with increasing heating rate due to the delayed transition with increasing rate. Evaluation of the different degrees of recovery, taken in the heating-rate dependent intermediate shapes, are depicted for 120, 150, and 170 °C representatively in Figure 2 (right) and reveal a strong dependence between the degree of recovery and heating rate in an even broader temperature range than that found for x-sPP.[17] This demonstrates that constrained quenched x-PET is capable of detecting heating rates. Thus, the approach to imprint heating rate-sensitive shape memory to fully amorphous quenchable semi-crystalline polymers is feasible.

Taking a look at the recovery of x-PET with a heating rate of 5 K min^{-1} (Figure 2 (left)) shows that the sample stops its retraction at 90 °C reaching a recovery of ≈30%. Further heating results in a decrease of the recovery to below 20% at 200 °C, i.e., the sample elongates in this temperature range. This is surprising because crystallization should lead to an increase in density and thus a further volume decrease. A possible explanation of

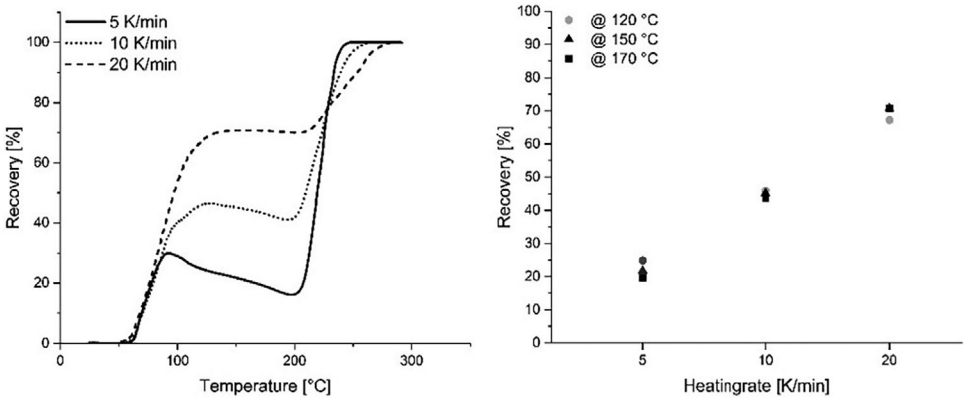

Figure 2. Degree of recovery versus temperature plots for different heating rates **(left)**. Degree of recovery at different temperatures as a function of the applied heating rate (**right**).

this could be the anisotropic crystallization of the samples with a high residual strain in the intermediate state. To confirm this thesis, structural and morphological analyses were performed on a sample, after heating with a heating rate of 5 K min^{-1} to a temperature of 150 °C and subsequent cooling to room temperature. To this end, wide/small angle X-ray scattering (WAXS/SAXS) and transmission electron microscopy (TEM) were carried out.

The recorded WAXS pattern shown in Figure 3 (top right) indicates that PET cold-crystallizes biaxially oriented in the known triclinic unit cell ($a = 0.8786$ nm, $b = 0.7733$ nm, $c = 0.3481$ nm) and that the formed crystals are responsible for stabilizing x-PET in its intermediate form. The SAXS pattern in Figure 3 (bottom left) indicates the formation of a stacked lamellar morphology and also confirms a biaxial orientation of the crystals.

The bright field transmission electron micrograph in Figure 3 (bottom right) confirms the stacked lamellar morphology of the x-PET sample in its intermediate shape. Due to imaging in phase contrast under negative defocus conditions lamellar crystals occur darker than amorphous regions. Both, the electron diffraction pattern as well as the Fast Fourier Transformation (FFT) in Figure 3 (bottom right) correspond to the respective WAXS and SAXS patterns, shown in Figure 3 (top right, bottom left). The crystals in the intermediate state indeed form highly oriented structures along the stretching direction, which explains the increase in length of the sample during further crystallization. A similar effect was observed for heating rate sensitive x-sPP[17] and is also known from cold-drawn films of PET.[26]

3. Conclusion

It was shown that the crosslinking of PET as a semi-crystalline, fully amorphous quenchable polymer is suitable for equipping it with a heating rate-dependent shape memory. The prepared x-PET networks are capable of reacting sensitively on heating rates ranging from 5 and to at least 20 K min^{-1} by stabilizing intermediate forms with degrees of recovery ranging from 20 to 70%, respectively. Higher heating rates could not be confirmed by the available DMA 850 (TA Instruments, Inc.). Thus, x-PET is only the second example of a heating-rate sensitive shape memory polymer, working by simultaneously addressing length retraction of a stretched amorphous polymer and simultaneously inducing crystallization when heating above Tg, but below Tm. Since both processes have different dynamics, the retraction is stopped by crystallization at different lengths depending on the heating rate. This novel concept of heating rate-sensitive smart materials will be broadened in future work focusing on other semi-crystalline polymers with tunable intermediate states for other temperature regions.

4. Experimental Section

Materials: PET (Arnite D02 300, M_w = 52 kg mol^{-1}[27]) was kindly provided by Akzo. Phthalic anhydride (PA, 99,9% purity, thermo scientific) and 4,4′-methylenebis (N,N-diglycidylaniline) (TGDDM, >98% purity, TCI) were used without further purification. Analytical-grade acetone was used for dissolving PA and TGDDM.

Network Synthesis: The synthesis was performed according to the literature[21] using 1 phr of PA and 3 phr TGDDM. To this end, the crosslinking agents were dissolved in acetone at room temperature. Thin strips of PET foil were added and stirred continuously until the acetone evaporated. The coated strips were processed in a twin screw extruder (HAAKE MiniLab 3 Micro-Compounder, Thermo Fisher Scientific, Inc.) at 250 °C and 60 rpm. Subsequently, the extrudate was granulated and compression molded to sheets of 0.5 mm thickness in a heating press at 270 °C, cured for 15 min at this temperature, and cut to rectangular samples of 30 mm length and 5 mm width after cooling to room temperature.

Sample Characterization: The netchain molecular weights M_c were calculated from the average Young's modulus taken at a temperature of 260 °C determined by a Dynamic Mechanical Analyzer (DMA 850, TA Instruments Inc.), according to Flory's theory of viscoelasticity[28] using Equation (1).

$$M_c = \frac{2\,(1+\nu)\cdot\rho\,(T)\cdot R\cdot T}{E\,(T)} \tag{1}$$

Here, $E(T)$ is the storage modulus, ν is the Poisson's ratio assumed to be 0.5, R is the universal gas constant (8.314 J mol K^{-1}), and T is the absolute temperature. The melt density of ρ(260 °C) = 1.18 g cm^{-3} was used according to reference.[21]

Glass transition temperature T_g, melting temperature T_m, crystallization temperature T_c, and the respective enthalpies ΔH_m and ΔH_c were determined using Differential Scanning Calorimetry (DSC 2910, TA Instruments Inc.) at a heating rate of 10 K min^{-1}. The total crystallinity was cal-

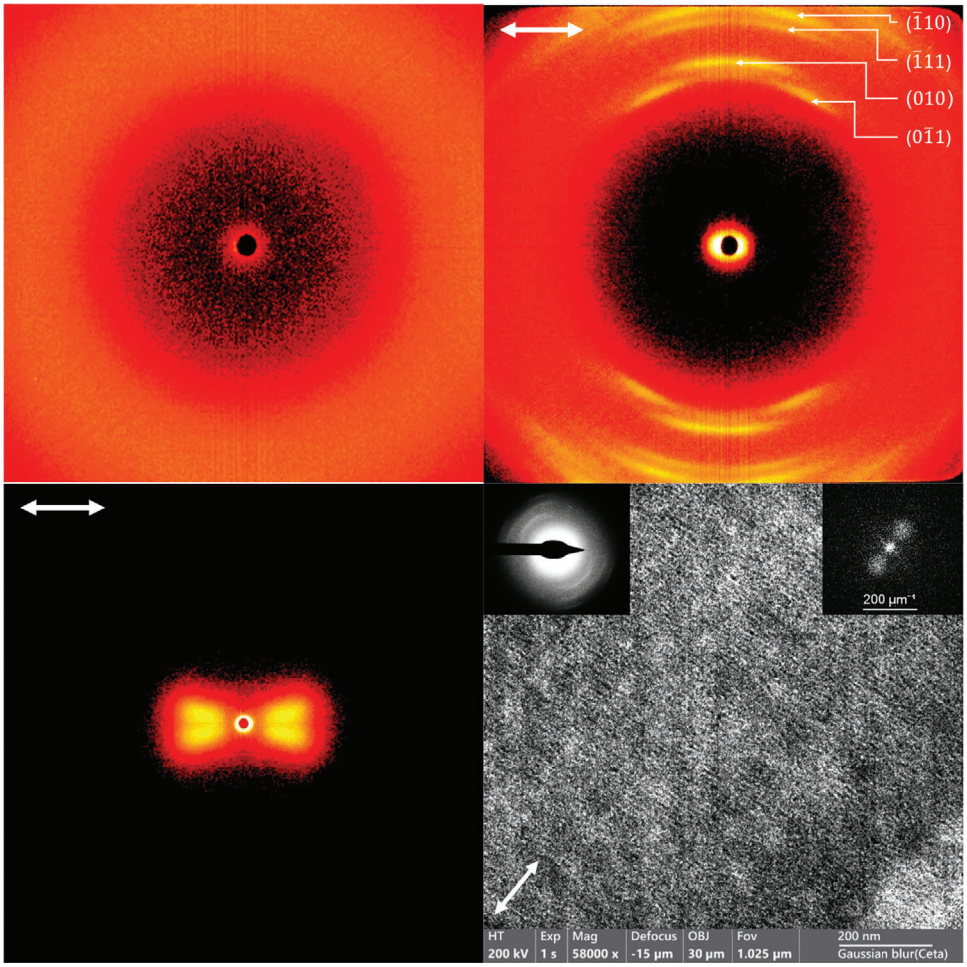

Figure 3. WAXS diffraction pattern of x-PET after stretching to a strain of 200% at a temperature of 290 °C and subsequent constrained quenching in ice water (**top left**). WAXS diffraction pattern of intermediate shape heated with 5 K min^{-1} to 150 °C **(top right)**, SAXS diffraction pattern of intermediate shape heated with 5 K min^{-1} to 150 °C **(bottom left)**, drawing direction indicated in the top left corner. Phase contrast TEM bright field image of a thin film cut from an x-PET sample heated to its intermediate shape at 150 °C with 5 K min^{-1} **(bottom right)**. The arrow indicates the stretching direction of the molten x-PET before quenching. The electron diffraction pattern and the Fast Fourier Transformation are shown in the upper left and right corner, respectively.

culated as the ratio of measured melting enthalpy ΔH_m and heat of fusion $\Delta H_m{}^0$. $\Delta H_m{}^0$ of PET was assumed to be 136 J g^{-1}.[29]

Microstructural characterization was carried out by wide as well as small-angle X-ray-scattering (WAXS/SAXS) as well as transmission electron microscopy. WAXS/SAXS patterns were recorded using a VANTEC-2000 detector (Bruker AXS GmbH) and a micro-focus X-ray source (IμS, Incoatec GmbH) with Cu-anode and integrated Montel Optic operated at 50 kV and 0.600 mA. The X-ray wavelength was 0.15406 nm with a sample-to-detector distance of 13.25 cm and 109 cm, respectively. Data were accumulated for 900 s.

Transmission electron microscopy was performed on a Talos F200X G2 from Thermo Fisher Scientific, Inc. at an acceleration voltage of 200 kV. Thin films were prepared using an EM UC7 Ultramicrotome from Leica Microsystems GmbH and investigated without any staining under defocus conditions of ≈−15 µm.

Determination of Heating Rate Sensitivity: The PET samples were heated to 290 °C, stretched to a pre-determined maximal strain ϵ_{prog} of 200%[21] and quenched in ice water. The recovery process of the samples was derived from the length change of the samples recorded in dependence on temperature with a Dynamic Mechanical Analyzer DMA 850 (TA Instruments Inc.) operated with heating rates of 5, 10, and 20 K min^{-1} while applying a constant force of 0.01 N. The degree of recovery $R_r(T)$ was calculated according to Equations (2) and (3) from L_{prog} and the temperature dependent length $L(T)$ during recovery. ϵ_{prog} was determined using marks on the sample. Since shorter pieces of the elongated samples needed to be mounted between the tension clamps, the fully recovered length (L_0) of the parts was calculated according to Equation (2) using the programmed strain ϵ_{prog} and the distance between the film clamps (L).

$$L_0 = \frac{L}{\epsilon_{prog} + 1} \tag{2}$$

$$R_r\ (T) = 1 - \frac{L\,(T) - L_0}{L_{prog} - L_0} \tag{3}$$

Acknowledgements

The authors acknowledge support from funding provided by the Deutsche Forschungsgemeinschaft DFG under Grant TI 326/8-1. The TEM was in part financed by the DFG under Grant INST 212/423-1 FUGG.

Open access funding enabled and organized by Projekt DEAL.

Conflict of Interest

The authors declare no conflict of interest.

Data Availability Statement

The data that support the findings of this study are available from the corresponding author upon reasonable request.

Keywords

cross-linked PET, crystallization, predictive material, shape memory

Received: May 14, 2024
Revised: July 23, 2024
Published online: August 13, 2024

[1] M. A. C. Stuart, W. T. S. Huck, J. Genzer, M. Muller, C. Ober, M. Stamm, G. B. Sukhorukov, I. Szleifer, V. V. Tsukruk, M. Urban, F. Winnik, S. Zauscher, I. Luzinov, S. Minko, *Nat. Mater.* **2010**, *9*, 101.
[2] F. Li, W. Zhu, X. Zhang, C. Zhao, M. Xu, *J. Appl. Polym. Sci.* **1999**, *71*, 1063.
[3] D. Segiet, T. Raidt, H. Özdem, S. Weckes, J. C. Tiller, F. Katzenberg, *J. Polym. Sci., Part B: Polym. Phys.* **2019**, *57*, 1053.
[4] H. M. Jeong, S. Y. Lee, B. K. Kim, *J. Mater. Sci.* **2000**, *35*, 1579.
[5] T. J. White, D. J. Broer, *Nat. Mater.* **2015**, *14*, 1087.
[6] Z. M. Png, C.-G. Wang, J. C. C. Yeo, J. J. C. Lee, N. E. Surat'man, Y. L. Tan, H. Liu, P. Wang, B. H. Tan, J. W. Xu, *Mol. Syst. Design Eng.* **2023**, *8*, 1097.
[7] Y. Takashima, S. Hatanaka, M. Otsubo, M. Nakahata, T. Kakuta, A. Hashidzume, H. Yamaguchi, A. Harada, *Nat. Commun.* **2012**, *3*, 1270.
[8] S. Ikejiri, Y. Takashima, M. Osaki, H. Yamaguchi, A. Harada, *J. Am. Chem. Soc.* **2018**, *140*, 17308.
[9] J. Keyvan Rad, Z. Balzade, A. R. Mahdavian, *J. Photochem. Photobiol., C* **2022**, *51*, 100487.
[10] K. Schöller, S. Küpfer, L. Baumann, P. M. Hoyer, D. de Courten, R. M. Rossi, A. Vetushka, M. Wolf, N. Bruns, L. J. Scherer, *Adv. Funct. Mater.* **2014**, *24*, 5194.
[11] R. Hoeher, T. Raidt, N. Novak, F. Katzenberg, J. C. Tiller, *Macromol. Rapid Commun.* **2015**, *36*, 2042.
[12] R. Hoeher, T. Raidt, M. Rose, F. Katzenberg, J. C. Tiller, *J. Polym. Sci., Part B: Polym. Phys.* **2013**, *51*, 1033.
[13] D. Quitmann, N. Gushterov, G. Sadowski, F. Katzenberg, J. C. Tiller, *Adv. Mater.* **2014**, *26*, 3441.
[14] A. Lendlein, H. Y. Jiang, O. Junger, R. Langer, *Nature* **2005**, *434*, 879.
[15] H. Y. Jiang, S. Kelch, A. Lendlein, *Adv. Mater.* **2006**, *18*, 1471.
[16] B. Heuwers, D. Quitmann, F. Katzenberg, J. C. Tiller, *Macromol. Rapid Commun.* **2012**, *33*, 1517.
[17] R. Hoeher, T. Raidt, F. Katzenberg, J. C. Tiller, *ACS Appl. Mater. Interfaces* **2016**, *8*, 13684.
[18] T. Raidt, R. Hoeher, F. Katzenberg, J. C. Tiller, *Macromol. Rapid Commun.* **2015**, *36*, 744.
[19] T. Raidt, R. Hoeher, M. Meuris, F. Katzenberg, J. C. Tiller, *Macromolecules* **2016**, *49*, 6918.
[20] D. Quitmann, F. M. Reinders, B. Heuwers, F. Katzenberg, J. C. Tiller, *ACS Appl. Mater. Interfaces* **2015**, *7*, 1486.
[21] T. Raidt, M. Schmidt, J. C. Tiller, F. Katzenberg, *Macromol. Rapid Commun.* **2018**, *39*, 1700768.
[22] R. Sharma, D. P. Bisen, U. Shukla, B. G. Sharma, *Recent Res. Sci. Technol.* **2012**, *4*, 77.
[23] R. Hoeher, T. Raidt, C. Krumm, M. Meuris, F. Katzenberg, J. C. Tiller, *Macromol. Chem. Phys.* **2013**, *214*, 2725.
[24] T. Xie, *Nature* **2010**, *464*, 267.
[25] M. Behl, I. Bellin, S. Kelch, W. Wagermaier, A. Lendlein, *Adv. Funct. Mater.* **2009**, *19*, 102.
[26] W. J. Dulmage, A. L. Geddes, *J. Poly. Sci.* **1958**, *31*, 499.
[27] Y. Dirix, H. Jagt, R. Hikmet, C. Bastiaansen, *J. Appl. Phys.* **1998**, *83*, 2927.
[28] P. J. Flory, *Principles of Polymer Chemistry*, Cornell University Press, Ithaca, NY **1953**.
[29] H. W. Starkweather Jr., P. Zoller, G. A. Jones, *J. Polym. Sci.: Polym. Phys. Ed.* **1983**, *21*, 295.

